

$^{89}\text{Y}(^3\text{He}, t)$ reaction at 25 MeV[†]

M. Stautberg Greenwood and M. Pluta

*De Paul University, Chicago, Illinois 60614
and Argonne National Laboratory, Argonne, Illinois 60439*

N. Anantaraman*

Argonne National Laboratory, Argonne, Illinois 60439

L. R. Greenwood

*Northwestern University, Evanston, Illinois 60201
and Argonne National Laboratory, Argonne, Illinois 60439*

(Received 26 August 1974)

Nineteen angular distributions were obtained for the $^{89}\text{Y}(^3\text{He}, t)^{89}\text{Zr}$ reaction at 25 MeV. The angular distribution of the 0.59-MeV state, thought previously to be the antianalog state, is characterized by $L = 2$ with spin-flip. This indicates the presence of a configuration, other than the antianalog configuration, in the wave function of the 0.59-MeV state. Arguments are presented to show that the $g_{9/2} \rightarrow g_{7/2}$ transition with $L = 2, S = 1$ is responsible for the excitation of this state. Angular distributions leading to the ground state, the 1.514-, 2.784-, and 2.932-MeV states are very similar. Since the ground state and the 1.514-MeV state have $J^\pi = \frac{9}{2}^+$, this suggests that the other states also have $J^\pi = \frac{9}{2}^+$. The angular distribution leading to the ground state was not satisfactorily fitted by distorted-wave calculations, since the forward peaking corresponded to $L = 2$, rather than to the allowed $L = 3$ and $L = 5$. The structure of the $\frac{9}{2}^+$ states was investigated in terms of the coupling of a $g_{9/2}$ neutron hole to the 0^+ states in ^{90}Zr .

[NUCLEAR REACTIONS $^{89}\text{Y}(^3\text{He}, t), E = 25$ MeV; measured $\sigma(\theta)$. DWBA analysis. ^{89}Zr deduced levels, l, π .]

I. INTRODUCTION

The $^{89}\text{Y}(^3\text{He}, t)^{89}\text{Zr}$ reaction was studied concurrently with the $^{41}\text{K}(^3\text{He}, t)^{41}\text{Ca}$ reaction.¹ These target nuclei were chosen because of similar shell-model characteristics, which are illustrated in Fig. 1. Both have an odd number of protons, resulting in a proton hole, and an even number of neutrons. Thus, the $(^3\text{He}, t)$ reaction to the ground state completes the proton shell. Also, both target nuclei have two unfilled proton shells, which plays an important role in interpreting transitions to antianalog states.

The $^{89}\text{Y}(^3\text{He}, t)$ reaction is also of interest because it is one of the several charged-particle reactions which can be used to study ^{89}Zr . At present information about ^{89}Zr (Ref. 2) is obtained from the $^{90}\text{Zr}(p, d)$ reaction,³ the $^{90}\text{Zr}(^3\text{He}, \alpha)$ reaction,^{4, 5} the $^{91}\text{Zr}(p, t)$ reaction,^{6, 7} and the $^{89}\text{Y}(^3\text{He}, t)$ reaction at a bombarding energy of 33 MeV.⁸ Information about the ^{89}Zr levels is also obtained from the positron decay of ^{89}Nb (Ref. 9) and from γ -decay studies using the $^{90}\text{Zr}(\alpha, \alpha' n\gamma)^{89}\text{Zr}$ reaction¹⁰ and the $^{89}\text{Y}(p, n\gamma)$ reaction.^{11, 12}

II. EXPERIMENTAL PROCEDURES

The experimental setup and data analysis procedures were the same as described for the $^{41}\text{K}(^3\text{He}, t)$ reaction.¹ The tritons were detected using Kodak NTB emulsions. The ^{89}Y target thickness was $250 \mu\text{g}/\text{cm}^2$, which resulted in a resolution of about 38 keV. A sample spectrum, along with fits to the peaks, is shown in Fig. 2.

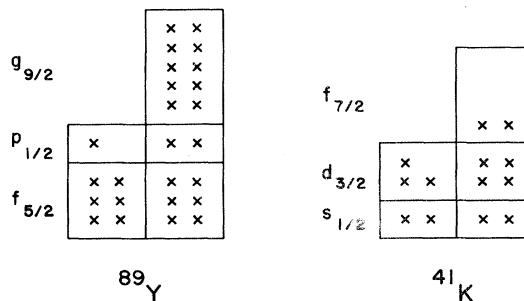


FIG. 1. Comparison of the shell-model structure of ^{89}Y and ^{41}K .

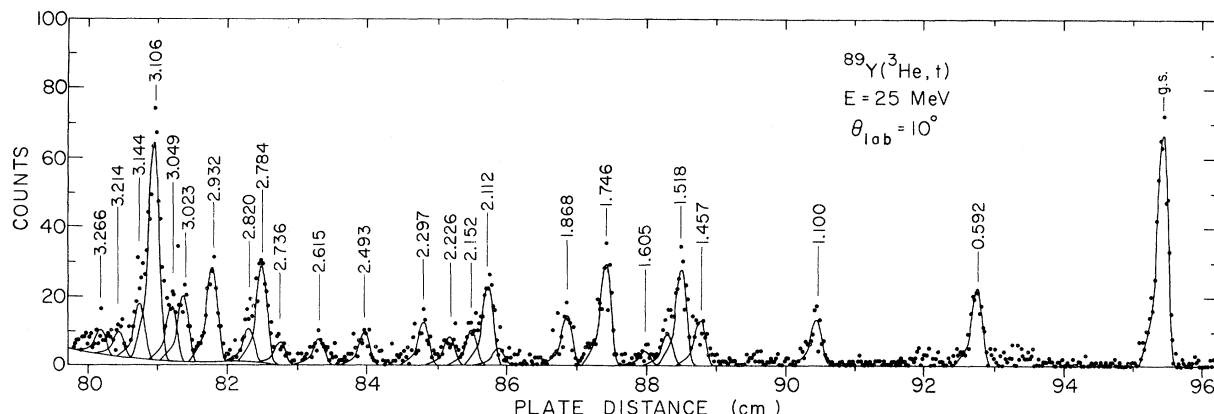


FIG. 2. Spectrum obtained using emulsions and analysis from program AUTOFIT.

III. RESULTS AND DISCUSSION

The optical-model parameters^{13, 14} used in the distorted-wave (DW) calculations are listed in Table I. The single-particle wave functions were generated from a potential having a radius of $1.2A^{1/3}$ fm and a diffuseness of 0.7 fm. A Yukawa potential with a reciprocal range of 1 fm^{-1} was used for the interaction between the ^3He projectile and the target neutron. Calculations were carried out for the $g_{9/2} \rightarrow g_{9/2}$ transition with $L=2$ and 4 for $\alpha=0.5, 0.7, 1.0$, and 1.4 fm^{-1} . The results, shown in Fig. 3, demonstrate that the angular position of the first maximum does not depend upon α and that the angular momentum transfer L can be determined by using DW calculations with $\alpha = 1 \text{ fm}^{-1}$. The results are summarized and compared with other data in Table II.

A. Structure of the 0.59-MeV state in ^{89}Zr

The $\frac{1}{2}^-$ antianalog of the ^{89}Y ground state is obtained by the replacement of a $p_{1/2}$ or a $g_{9/2}$ neutron in ^{89}Y with a proton in the same orbit. The state at 0.59 MeV in ^{89}Zr has been identified by Hinrichs and Trentelman⁸ as the $\frac{1}{2}^-$ antianalog state. Since the $^{90}\text{Zr}(p, d)$ reaction populates the 0.59-MeV state by the pickup of a $p_{1/2}$ neutron,

TABLE I. Optical-model parameters.

	V_R (MeV)	r_R (fm)	a_R (fm)	V_I^a (MeV)	r_I (fm)	a_I (fm)
$^{89}\text{Y} + ^3\text{He}^b$	175.1	1.14	0.723	14.88	1.60	0.81
$^{89}\text{Zr} + t^c$	170.2	1.16	0.739	18.8	1.52	0.751

^a Indicates a volume potential.

^b Reference 13.

^c Reference 14.

the identification of this state as the antianalog state is quite reasonable. By definition, the $(^3\text{He}, t)$ reaction leading to an antianalog state must occur without spin-flip ($S=1$). From angular momentum considerations, the transition in the $^{89}\text{Y}(^3\text{He}, t)$ reaction leading to the $\frac{1}{2}^-$ state at 0.59 MeV in ^{89}Zr can occur with $L=0$ and $L=2$, but $L=2$ requires spin-flip. Therefore, if the 0.59-MeV state is correctly identified as the antianalog state, then spin-flip transitions are not allowed and the angular distribution of the 0.59-MeV state is expected to have an $L=0$ shape. However, the angular distribution of the 0.59-MeV state, shown in Fig. 4, is characterized by $L=2$, not by $L=0$. French and Macfarlane¹⁵ have shown that the excitation of the antianalog state may be very weak when the target nucleus in the charge-exchange

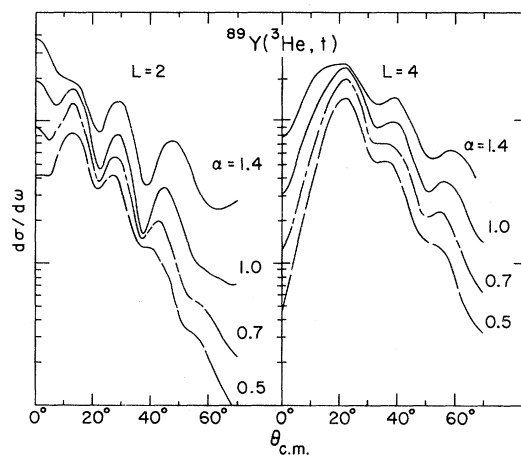


FIG. 3. The effects of varying the reciprocal range parameter α are shown for the $g_{9/2} \rightarrow g_{9/2}$ transition with $L=2$ and 4. The placement of the DW calculations, plotted on a semilogarithmic scale, permits comparison of the curves but does not indicate the relative magnitude of the angular distributions.

TABLE II. Summary of data and comparison with previous results.

E_x (MeV)	Error (keV)	This work		Previous ^a results		(p, d) l_n^b
		L	J^π	J^π	E	
0		3	+	$\frac{3}{2}^+$	0	4
0.592	4	2	-	$\frac{1}{2}^-$	0.588	1
1.100	4	2	-	$\frac{3}{2}^-$	1.095	1
1.456	6	2	-	$\frac{5}{2}^-$	1.452	3
1.518	6	3	+	$\frac{3}{2}^+$	1.512	
1.605	17			$\frac{5}{2}^+$	1.628	
1.746	9	2	-	$\frac{3}{2}^-$	1.743	
1.868	6	2	-	$\frac{3}{2}^-$	1.865	1
2.112	12			$\frac{7}{2}^-$, $\frac{5}{2}^-$	2.102	3
2.152	12	4	-			
2.226	7	4	-	$(\frac{11}{2}^+)$	2.221	
2.297	8	4	-	$\frac{7}{2}^-$	2.300	
2.493	11					
2.585	11			$(\frac{3}{2}^-)$	2.570	
2.615	7	(6)		$\frac{7}{2}^-$	2.613	
2.736	9	4	-	$(\frac{7}{2}^+)$	2.755	4
2.784	15	3	$(\frac{3}{2}^+)$			
2.820	9	4	-			
2.906	9				2.891	
2.932	9	3	$(\frac{3}{2}^+)$		2.926	
3.023	7			$\frac{7}{2}^-$	3.017	3
3.049	7	4	-			
3.106	4	2	-	$(\frac{7}{2}^+)$	3.094	
3.144	19					
3.214	13	4	-			
3.266	10					
3.524	10					

^a Obtained from Refs. 1, 6, 11, and 12.^b References 3 and 4.

reaction has two unfilled proton shells. [This fact has also been used in interpreting the data from the $^{41}\text{K}(^3\text{He}, t)$ reaction.] Since the angular distribution has $L=2$, this shows that the excitation of the 0.59-MeV state is not due to the antianalog configuration. A likely possibility is that the $p_{1/2} \rightarrow p_{1/2}$ and/or the $g_{9/2} \rightarrow g_{9/2}$ transitions occurring with $L=2$ and $S=1$ are responsible for the excitation. The effects of a tensor force are known to play a very important role in spin-flip transitions.¹⁶ Distorted-wave calculations, including the tensor contribution, predict a larger cross section for $L=2$ and $S=1$ than for $L=0$ and $S=1$

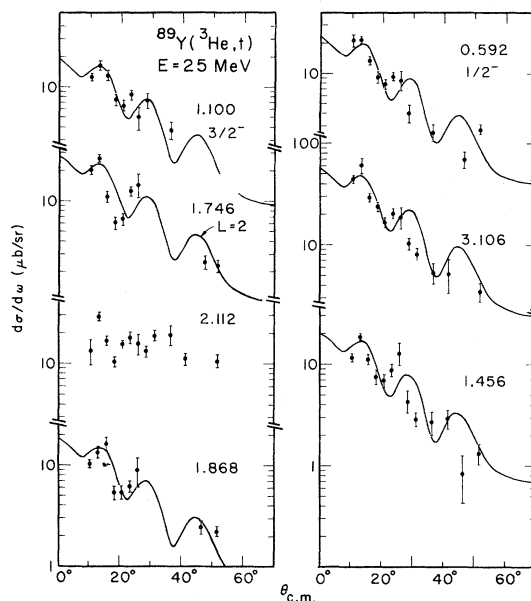
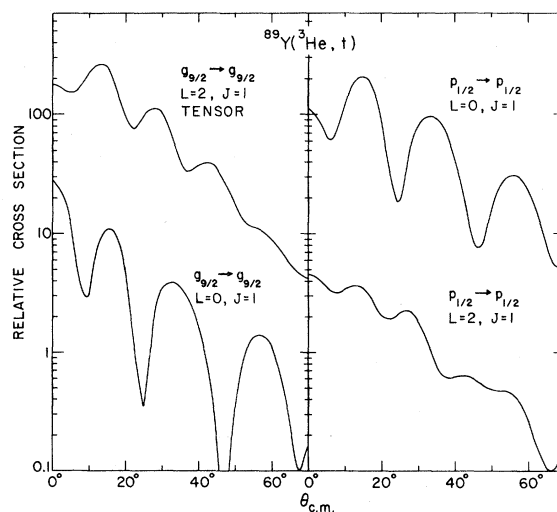


FIG. 4. Comparison of angular distributions with DW calculations.

for the $g_{9/2} \rightarrow g_{9/2}$ transition, while the reverse is true for the $p_{1/2} \rightarrow p_{1/2}$ transition. The results for the tensor force are shown in Fig. 5. Therefore, these results suggest that the $[(\pi g_{9/2} \nu g_{9/2}^{-1})_1 (\pi p_{1/2})_{1/2}]_{1/2}$ configuration contributes to the wave function of the 0.59-MeV state. The amount of this configuration could be determined if an accurate interaction potential between the protons in the ^3He projectile and the target neutron were known. Normalizing the DW calculation

FIG. 5. DW calculations showing the effect of the tensor force for the $g_{9/2} \rightarrow g_{9/2}$ and the $p_{1/2} \rightarrow p_{1/2}$ transitions with $L=0$, $S=1$, and $L=2$, $S=1$.

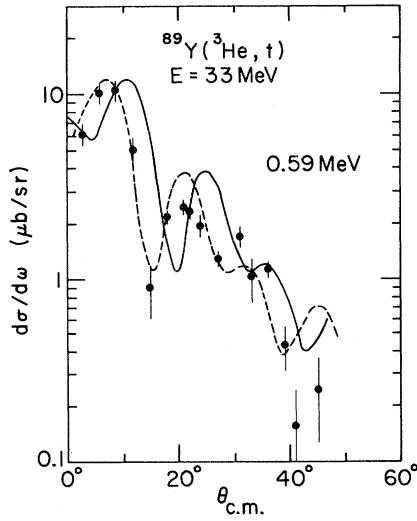


FIG. 6. Comparison of the $^{89}\text{Y}({}^3\text{He}, t)$ reaction at 33 MeV with DW calculations for $L=2$. The solid curve is the actual calculation, while the dashed curve results from an angular shift of 4° .

to the data would yield $V_0^2 a^2$, where V_0 is the potential well depth and “ a ” is the coefficient of this configuration in the wave function.

Hinrichs and Trentelman⁸ have studied the $^{89}\text{Y}-({}^3\text{He}, t)$ reaction at 33 MeV. The angular distribution for the 0.59-MeV state at 33 MeV is fitted best with $L=1$, whereas the present data indicate $L=2$. One possible explanation is that the data at 33 MeV manifest the angular shift noted previously¹⁷ when data and DW calculations are compared. The data are compared in Fig. 6 with DW calculation for a $g_{9/2}-g_{9/2}$, $L=2$ transition using optical-model parameters listed in Table I. The solid curve shows the actual calculation, while the dashed curve results from an angular shift of 4° . This amount of angular shift has been reported by Comfort *et al.*¹⁷ when $({}^3\text{He}, t)$ angular distributions

for the $\frac{1}{2}^-$ states can be expressed as follows

$$|E, \frac{1}{2}^- \rangle = \beta_1 |(\pi g_{9/2} \nu g_{9/2}^{-1})_0 (\pi p_{1/2}) \rangle + \beta_2 |(\pi g_{9/2} \nu g_{9/2}^{-1})_1 (\pi p_{1/2}) \rangle + \beta_3 |(\pi p_{1/2})_0^2 (\nu p_{1/2}^{-1}) \rangle + \beta_4 |(\pi g_{9/2})_0^2 (\nu p_{1/2}^{-1}) \rangle. \quad (3)$$

TABLE III. Wave functions and energy levels for $\frac{1}{2}^-$ states. ^a

E	T	α_1	α_2	α_3	α_4	β_1	β_2	β_3	β_4	$ \langle \text{AAS} E \rangle ^2$
0.57	5	0.35	0.1	0.89	0.29	-0.19	-0.31	-0.55	-0.75	34%
1.86	5	-0.50	-0.27	0.04	0.82	-0.19	-0.54	-0.52	0.64	31%
5.32	5	-0.28	-0.80	0.34	-0.41	-0.33	0.78	-0.51	0.13	34%
8.08	6	0.74	-0.53	-0.31	0.26	0.90	0.10	-0.41	0.03	1%

^a Reference 19.

leading to states of known spin and parity are compared with DW calculations. Thus, when the angular shift is taken into account, the data at 33 MeV can also be interpreted in terms of a $g_{9/2}-g_{9/2}$ transition with $L=2$ and $S=1$. However, it is indeed very difficult to understand why the DW calculation is successful in fitting the forward angle behavior of the angular distribution at 25 MeV, but requires a shift of 4° at 33 MeV.

Recently Gloeckner and Serduke¹⁸ have investigated the shell-model structure of $N=50$ nuclei resulting from the proton configurations $(2p_{1/2}, 1g_{9/2})^n$. These studies are presently being extended to investigate the structure of ^{89}Zr (Ref. 19) arising from the coupling of a neutron hole to states in ^{90}Zr . Configurations in ^{89}Zr having $J^\pi = \frac{1}{2}^-$ result from the coupling of a $g_{9/2}$ neutron hole to the 4^- and 5^- states in ^{90}Zr and from the coupling of a $p_{1/2}$ neutron hole to the 0^+ ground state and excited state at 1.75 MeV in ^{90}Zr . The 4^- and 5^- states in ^{90}Zr are due to the $(p_{1/2}g_{9/2})$ proton configuration, and the two 0^+ states from a mixing of the $(p_{1/2})^2$ and $(g_{9/2})^2$ proton configurations. The wave functions for the four states having $J^\pi = \frac{1}{2}^-$ are given as follows:

$$|E, \frac{1}{2}^- \rangle = \alpha_1 |5^- \times g_{9/2}^{-1} \rangle + \alpha_2 |4^- \times g_{9/2}^{-1} \rangle + \alpha_3 |0_{g.s.}^+ \times p_{1/2}^{-1} \rangle + \alpha_4 |0_{1.75}^+ \times p_{1/2}^{-1} \rangle. \quad (1)$$

The wave function for the antianalog state is given by

$$|\text{AAS}, \frac{1}{2}^- \rangle = \frac{1}{\sqrt{11}} |(\pi g_{9/2} \nu g_{9/2}^{-1})_0 (\pi p_{1/2}) \rangle - \sqrt{\frac{10}{11}} |(\pi p_{1/2})_0^2 (\nu p_{1/2}^{-1}) \rangle. \quad (2)$$

In order to facilitate comparison with the antianalog state, Eq. (1) should be expressed in the same system of basis states as Eq. (2). Following angular momentum recoupling, the wave function

The configurations of the first and third terms in Eq. (3) are the same as those found in Eq. (2). The values of α and β are given in Table III, which shows that the largest contribution to the wave function of the 0.59-MeV state is due to the $[(\pi g_{9/2})_0^2(\nu p_{1/2}^{-1})]$ configuration, and *not* to the configurations contained in the antianalog state. The amount of the antianalog configuration in each state can be found by calculating the overlap integral $\langle \text{AAS}, \frac{1}{2}^- | E, \frac{1}{2}^- \rangle$, using Eqs. (2) and (3). The square of the overlap integral, expressed in percentages, is given in Table III, which shows that the antianalog state is almost equally divided between the three $T=5$ states.

As discussed earlier, the excitation of the 0.59-MeV state in the $^{89}\text{Y}(^3\text{He}, t)$ reaction is due primarily to the $g_{9/2} \rightarrow g_{9/2}$ transition with $L=2$ and $S=1$. This transition leads to the $[(\pi g_{9/2}\nu g_{9/2}^{-1})_1(\pi p_{1/2})]$ configuration of the 0.59-MeV state. The shell-model calculations show a 10%

contribution of this configuration to the 0.59-MeV state.

In summary, there are several pieces of evidence which show that the state at 0.59 MeV cannot be identified as a pure antianalog state. First, the $^{89}\text{Y}(^3\text{He}, t)$ reaction leading to this state proceeds with spin-flip, which indicates the presence of a configuration other than the antianalog configuration. Secondly, shell-model structure studies show that the antianalog state is equally divided among three excited states.

B. States with $J^\pi = \frac{9}{2}^+$

Figure 7 shows four angular distributions which have the same characteristic shape. Both the ground state and the state at 1.518 MeV are known to have $J^\pi = \frac{9}{2}^+$. On this basis it seems very likely that the states at 2.784 and 2.932 MeV also have $J^\pi = \frac{9}{2}^+$. A state at 2.76 MeV is observed with $l_n = 4$ in the (p, a) reaction,⁴ lending support to the $J^\pi = \frac{9}{2}^+$ assignment.

The $g_{9/2} \rightarrow p_{1/2}$ transition to the ground state of ^{89}Zr requires $L=3$ and $L=5$, but $L=3$ must occur with spin-flip. Due to the peaking at forward angles, the data are more indicative of $L=3$ than of $L=5$. However, the $L=3$ DW calculation shows extremely poor agreement with the data at angles below 20° . The data also show more structure than the $L=3$ DW calculation. The experimental angu-

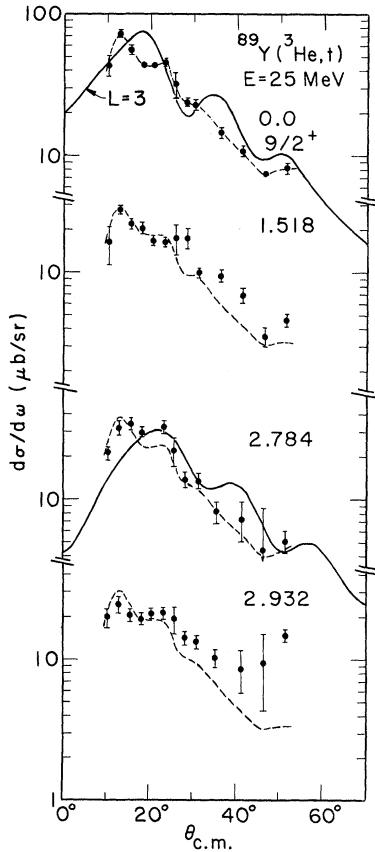


FIG. 7. The dashed curve is a visual fit through the data points of the ground-state angular distribution and the shape of the dashed curve is compared with the other angular distributions. The solid-line curves result from DW calculations for $L=3$.

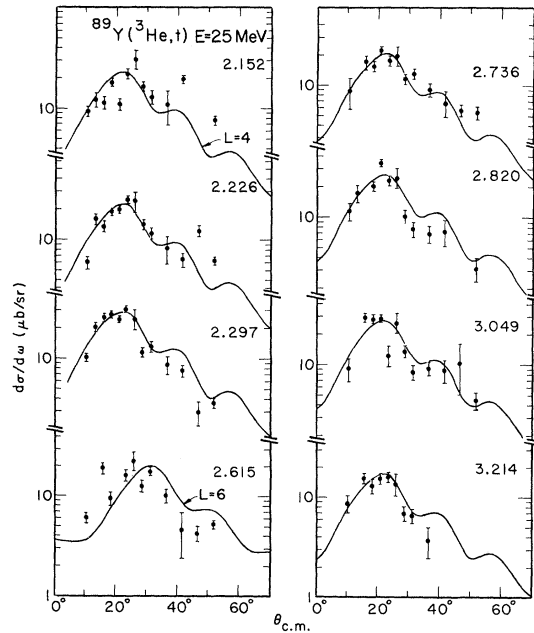


FIG. 8. Comparison of angular distributions having $L \geq 4$.

lar distribution peaks at about 12.5° , which is also the angle where $L=2$ DW calculations peak. A similar type of behavior has been noted in the $^{89}\text{Y}(^3\text{He}, t)$ reaction at 33 MeV. A satisfactory fit to the data was not found, but the forward angle peaking was indicative of $L=2$. Perhaps these results are a manifestation of a more complex mechanism for the $(^3\text{He}, t)$ reaction. Schaeffer and Bertsch²⁰ have shown that angular distributions arising from $0^+ \rightarrow 0^+$ transitions can be fitted with calculations which include the effects of the pickup-stripping mechanism. The results are very similar to the standard DW calculation with $L=1$, rather than $L=0$.

States with $J^\pi = \frac{9}{2}^+$ may be excited in the $^{89}\text{Y}(^3\text{He}, t)$ reaction by the $g_{9/2} \rightarrow p_{1/2}$ and $p_{1/2} \rightarrow g_{9/2}$ transitions. The antianalog of the 0.91-MeV state in $^{89}\text{Y}(J^\pi = \frac{9}{2}^+)$ can be excited only by the $p_{1/2} \rightarrow g_{9/2}$ transition. The state at 1.518-MeV in ^{89}Zr may be this antianalog state.⁸ Lieb and Hausmann¹¹ have suggested that $\frac{9}{2}^+$ states can be formed by the coupling of a $g_{9/2}$ neutron hole to the two 0^+ states in ^{90}Zr . The 0^+ ground state and the 1.75-MeV state in ^{90}Zr are due to a mixed configuration of two protons occupying the $p_{1/2}$ and $g_{9/2}$ orbits with a closed shell of 50 neutrons. These $\frac{9}{2}^+$ states in ^{89}Zr can be reached only by the $g_{9/2} \rightarrow p_{1/2}$ transition.

C. Other states

Angular distributions having $L \geq 4$ are shown in Fig. 8. The excitation may be due to the $g_{9/2} \rightarrow g_{9/2}$ transition proceeding by $L=4$ with or without spin-flip. The coupling with the $p_{1/2}$ proton hole leads to four states having $L=4$. The $f_{5/2} \rightarrow p_{1/2}$ transition also gives rise to $L=4$. The state at 2.226 MeV is tentatively assigned $J^\pi = \frac{11}{2}^+$ (Ref. 11). However, the $L=4$ assignment indicates negative parity. A spin of $\frac{11}{2}$ can be reached only with spin-flip.

States having $l_n=3$ in the $^{90}\text{Zr}(p, d)$ reaction^{3, 4} may be due to the $f_{5/2} \rightarrow p_{1/2}$ transition and those with $l_n=1$ to the $p_{3/2} \rightarrow p_{1/2}$ transition.

A state at 1.605 MeV was very weakly excited in this study. This state was observed with $l_n=2$ in the (p, d) reaction, indicating a 2.5% admixture of the $[(\nu g_{9/2})^{-2}(\nu d_{5/2})^2]$ configuration in the ground state of ^{90}Zr . The observation of this state in the $(^3\text{He}, t)$ reaction is evidence of the nonclosure of the $g_{9/2}$ shell in ^{89}Y , and corresponds to the replacement of a $d_{5/2}$ neutron in ^{89}Y by a $p_{1/2}$ proton.

The authors wish to thank F. J. D. Serduke for making the results of the shell-model study of ^{89}Zr available before publication and for several informative discussions.

[†]Work performed under the auspices of the U. S. Atomic Energy Commission.

*Presently at Nuclear Structure Research Laboratory, University of Rochester, Rochester, New York 14627.

¹M. Stautberg Greenwood, M. Pluta, L. R. Greenwood, and N. Anantaraman, preceding paper, Phys. Rev. C **11**, 1983 (1975).

²M. W. Johns, J. Y. Park, S. M. Shafroth, D. M. VanPatter, and K. Way, Nucl. Data **A8**, 373 (1970).

³J. B. Ball and C. B. Fulmer, Phys. Rev. **172**, 1199 (1968).

⁴H. Taketani, M. Adachi, Y. Yoshida, M. Ogawa, and K. Ashibe, Phys. Lett. **27B**, 499 (1968).

⁵C. M. Fou, R. W. Zurmühle, and J. M. Joyce, Phys. Rev. **155**, 1248 (1967).

⁶J. B. Ball, Phys. Rev. C **6**, 2139 (1972).

⁷T. Awaya *et al.*, J. Phys. Soc. Jpn. **32**, 1169 (1972).

⁸R. A. Hinrichs and G. F. Trentelman, Phys. Rev. C **4**, 2079 (1971).

⁹R. C. Hagenauer, Ph.D. thesis, University of Tennessee, 1969 (unpublished).

¹⁰A. Nilsson and M. Grecescu, Nucl. Phys. **A212**, 448 (1973).

¹¹K. P. Lieb and T. Hausmann, Phys. Rev. **186**, 1229 (1969).

¹²R. D. Gill, J. M. G. Caraca, A. J. Cox, and H. J. Rose, Nucl. Phys. **A187**, 369 (1972).

¹³E. F. Gibson, B. W. Ridley, J. J. Kraushaar, M. E. Rickey, and R. H. Bassel, Phys. Rev. **155**, 1194 (1967).

¹⁴E. R. Flynn, D. D. Armstrong, J. G. Beery, and A. G. Blair, Phys. Rev. **182**, 1113 (1969).

¹⁵J. B. French and M. H. Macfarlane, Phys. Lett. **2**, 255 (1962).

¹⁶E. Rost and P. D. Kunz, Phys. Lett. **30B**, 231 (1969).

¹⁷J. R. Comfort, J. P. Schiffer, A. Richter, and M. M. Stautberg, Phys. Rev. Lett. **26**, 1338 (1971).

¹⁸D. H. Gloeckner and F. J. D. Serduke, Nucl. Phys. (to be published).

¹⁹D. H. Gloeckner, R. D. Lawson, and F. J. D. Serduke (private communication).

²⁰R. Schaeffer and G. F. Bertsch, Phys. Lett. **38B**, 159 (1972).